Velocity Structure of Internal Tide Beams Emanating from Kaena Ridge, Hawaii

ANDY PICKERING AND MATTHEW H. ALFORD

Applied Physics Laboratory, University of Washington, Seattle, Washington

(Manuscript received 25 January 2012, in final form 13 March 2012)

ABSTRACT

Observations are reported of the semidiurnal (M_2) internal tide across Kaena Ridge, Hawaii. Horizontal velocity in the upper 1000–1500 m was measured during eleven ~240-km-long shipboard acoustic Doppler current profiler (ADCP) transects across the ridge, made over the course of several months. The M_2 motions are isolated by means of harmonic analysis and compared to numerical simulations using the Princeton Ocean Model (POM). The depth coverage of the measurements is about 3 times greater than similar past studies, offering a substantially richer view of the internal tide beams. Sloping features are seen extending upward north and south from the ridge and then downward from the surface reflection about ±40 km from the ridge crest, closely matching theoretical M_2 ray paths and the model predictions.

1. Introduction

Internal tides are the focus of active research because they are believed to supply a significant fraction of the energy required for deep-ocean mixing (Munk and Wunsch 1998; Wunsch and Ferrari 2004). In the immediate vicinity of supercritical topographic features, the generated waves take the form of compact beams propagating upward and downward from the ridge flanks. In the far field, the structure is dominated by the first and second vertical modes, presumably because the higher modes needed to form the beams dissipate because of their greater shear and slower propagation speeds. The transition between these two regimes is of interest because it provides information on the vertical and lateral structure of the dissipation in the vicinity of the ridge. The presence of low-frequency mesoscale flows modulates this picture in as-yet poorly understood ways, both by altering the stratification and therefore the location of the beams and by refraction from the horizontal structure and vertical shear of the currents (Rainville and Pinkel 2006).

The structure of M_2 internal tides in the vicinity of Hawaii's Kaena Ridge (Fig. 1) has been well documented in both models (e.g., Merrifield and Holloway 2002) and a host of observations made during the Hawaii Ocean Mixing Experiment (Rudnick et al. 2003). The models indicate generation at locations along the ridge flanks where the topographic slope equals the semidiurnal characteristic slope, subsequent upward propagation toward the surface, and downward propagation after that before finally becoming dominated by the lowest modes. As seen in depth-integrated energy flux (Fig. 1, colors), propagation is away from the ridge toward the north and south. In spite of hypotheses that the surface bounce might be a region of strong dissipation (New and Pingree 1992), no elevated dissipation was observed there (Lee et al. 2006).

By repeatedly steaming along long sections perpendicular to the ridge while measuring velocity and isopycnal depth in the upper few hundred meters with a shipboard acoustic Doppler current profiler (ADCP) and an undulating CTD, Martin et al. (2006) and Cole et al. (2009) confirmed elevated semidiurnal energy along the upward characteristics and in the vicinity of the surface bounce and downward radiation past that. Here, we build upon their work by presenting results from three recent cruises aboard R/V *Kilo Moana*, whose 38-kHz ADCP often reaches to 1500-m depth. The greater depth range of these measurements allows a substantially more detailed view of the beams than before. The observations are then compared with and found to be in good agreement with, the results of a 3D numerical model simulation. We introduce our measurements, present the results, and conclude with a brief discussion.

Corresponding author address: Andy Pickering, Applied Physics Laboratory, 1013 NE 40th St., Seattle, WA 98105.
E-mail: apickering@apl.washington.edu

DOI: 10.1175/JPO-D-12-018.1

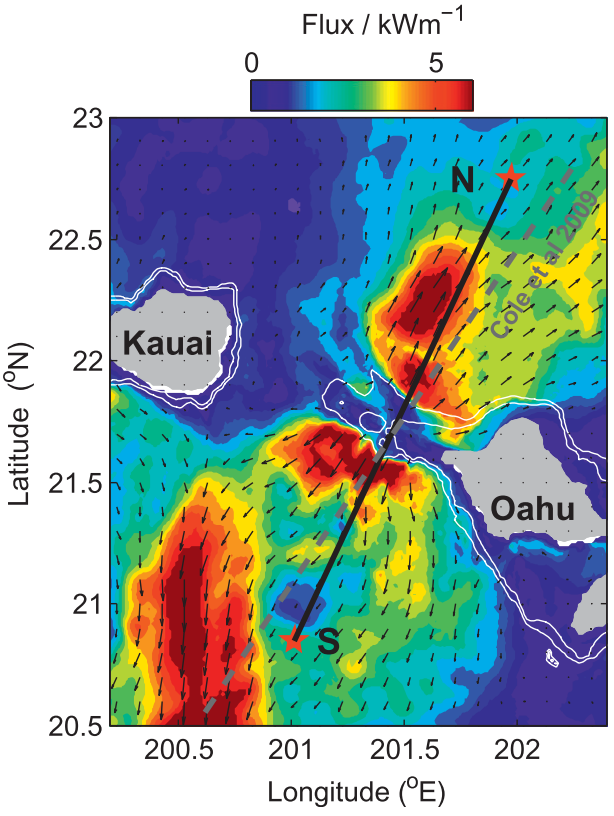

FIG. 1. Overview map of study area. Eleven shipboard ADCP transects were made along the black line from S to N. Depth-integrated M_2 energy flux magnitude (color) and vectors (black arrows) from numerical model simulations are plotted. The 1000- and 1500-m isobaths are contoured in white. The gray dashed line shows the approximate location of measurements made by Cole et al. (2009).

2. Data

a. Velocity

Observations are from three cruises conducted over a period of about 10 months (Table 1) while servicing a mooring located at Station Aloha (N, Fig. 1). Eleven transects (black line) were made, centered on and oriented approximately perpendicular to Kaena Ridge. The survey track was located along a region of strong semidiurnal internal tide energy flux, as evident from the numerical simulations (color and arrows).

Horizontal velocity was measured with a hull-mounted RDI Ocean Surveyor 38-kHz ADCP, operating with interlaced narrowband and broadband pings. The broadband pings have greater vertical resolution and somewhat higher precision. However, we use the narrowband pings because their range is substantially greater. Velocity was recorded in 24-m bins, with range during the transects varying from 1000 to 1500 m, depending on sea state and ship speed. The ship speed during the transects (10–12 kt) and the 5-min averaging interval of the ADCP data result in a horizontal resolution of 1.5–1.8 km. Data from all transects were linearly interpolated onto a uniform grid from waypoints S to N with 1.5-km horizontal spacing. Velocity was then rotated into an along-track (toward 25°T) and cross-track (toward 115°T) coordinate system.

TABLE 1. Dates of three cruises during which ADCP transects were made.

Cruise	Year	Dates	Transects
1	2010	29 Jun–4 Jul	1–4
2	2010	9–14 Oct	5–7
3	2011	3–5 Apr	8–11

b. Model

We compare our observations to numerical simulations from the Princeton Ocean Model (POM), kindly provided by L. Rainville et al. (2011, personal communication). Details of the model setup, which are similar to that of Merrifield and Holloway (2002), are described in Rainville et al. (2010). The model is forced with barotropic tidal currents and elevations of the M_2 tide from the TPXO6.2 global tide model (Egbert and Erofeeva 2002). The stratification is a 10-yr average of data from the Hawaii Ocean Time-Series and is uniform throughout the domain. Horizontal resolution is ~1 km and the model is run for 40 tidal cycles. A harmonic analysis is performed over the last six to extract M_2 components. Energy flux magnitude and vectors from the model are shown in Fig. 1. Horizontal velocity sections are compared with our observations in section 3.

3. Results

a. Individual sections

All 11 sections of measured along-track velocity are shown in Fig. 2. In addition to internal tides, measured velocity includes motion from a variety of processes, occurring at all resolved scales and time scales in the ocean at the time of each transect. However, many features in the raw data are clearly due to internal tides. These are first discussed in the context of the individual sections before isolating the M_2 motions in the next section with harmonic analysis.

Most sections show prominent sloping velocity features, tending to coincide with theoretical M_2 ray paths (dashed lines). These were computed from the equation

$$\frac{dz}{dx} = \sqrt{\frac{\omega^2 - f^2}{N(z)^2 - \omega^2}}, \tag{1}$$

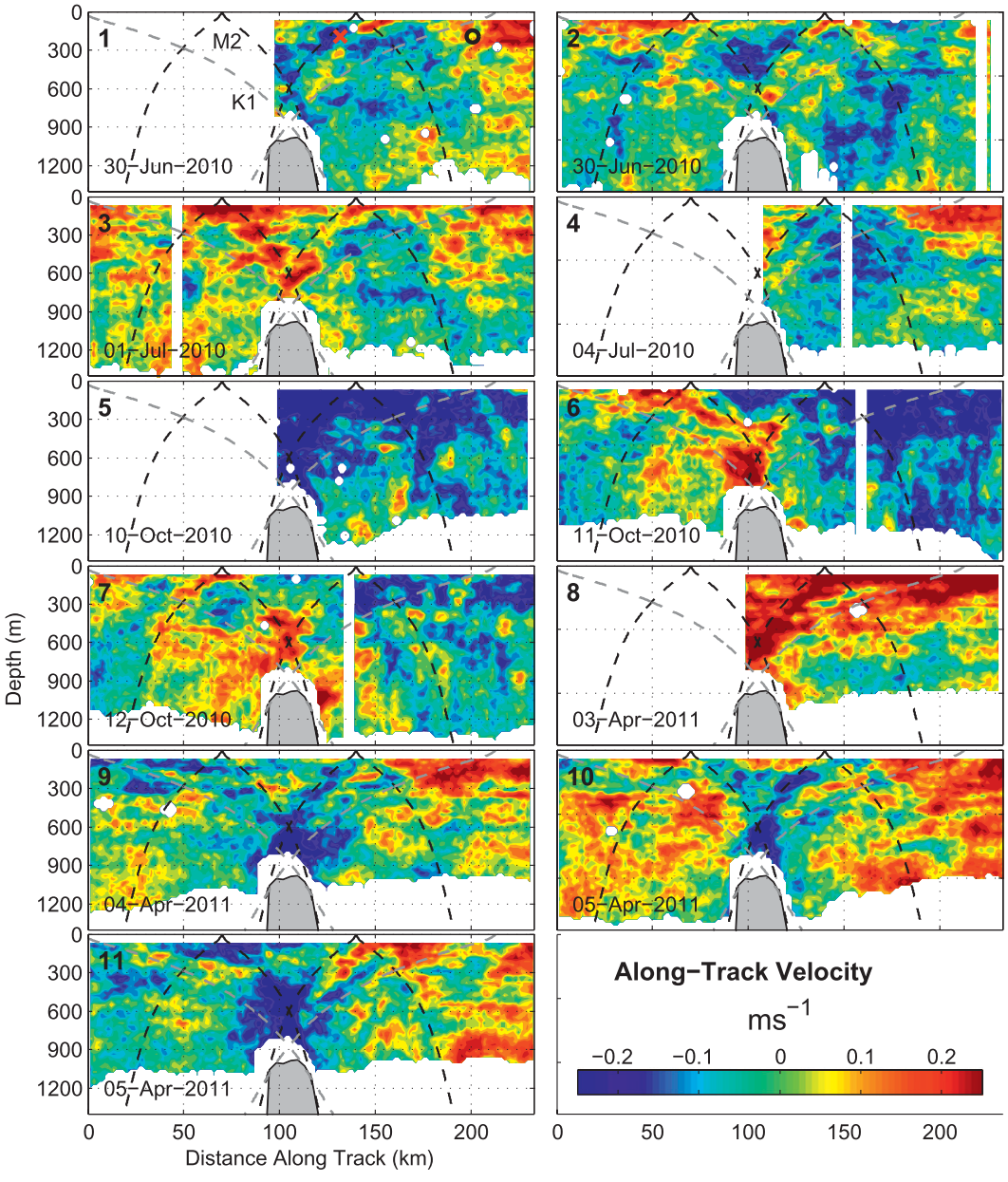

FIG. 2. Along-track component of raw velocity measured along each transect. Distance is measured from waypoint S to N (Fig. 1). Kaena Ridge (gray) is visible near the center of each transect. Theoretical M_2 (black dashed) and K_1 (gray dashed) ray paths are plotted emanating from supercritical locations of the ridge flanks. (top left) The locations of example time series 1 and 2 (Fig. 3) are indicated by the red x and black circle, respectively. The date of each transect is indicated in the bottom left of each panel.

where f is the Coriolis frequency, ω is the wave frequency, and N is the buoyancy frequency computed from the Levitus and Boyer (1994) climatology at 21°N, 201°E. Ray paths for semidiurnal (M_2) and diurnal (K_1) frequencies are plotted emanating from the locations of critical slopes on Kaena Ridge's flanks (ray paths are plotted at the same location in all plots). The steeper rays are associated with M_2.

Most sections show strong flow (relative to the background flow) just above the ridge between 600 and 900 m. Many also show stronger flow in the expected vicinity of the surface reflection of both the northward (e.g., sections 3 and 11) and southward beams (e.g., sections 3 and 7). To the north, the observed surface bounce appears to occur about 15–20 km northward of the expected locations given by the ray paths.

In addition to the semidiurnal beams, some features (e.g., section 2 south of the ridge or section 10 north of the ridge) have a shallower slope, roughly consistent with diurnal-frequency ray paths (gray dashed). These features may be K_1 internal tides generated at the ridge or possibly (½)M_2 waves resulting from parametric subharmonic instability (PSI; Carter and Gregg 2006).

b. Harmonic fit and model comparison

The individual transects are imperfect views of the semidiurnal tide because (i) they contain all frequencies and (ii) they are not synoptic snapshots because each took 12–13 h to complete. Martin et al. (2006) and Cole et al. (2009) intentionally detuned their observations from the M_2 frequency, such that a simple time average at each location was equivalent to a phase average. Because our sampling was opportunistic and our resulting phase coverage (Fig. 3a) is therefore variable and not as complete, we isolate semidiurnal motions with harmonic analysis at each along-track location.

More transects were completed on the northern side of the ridge than on the south. However, some of the extra transects are at similar M_2 phases, resulting in similar phase coverage at all locations. At each along-track location and depth with more than six occupations, M_2 amplitude u_0 and phase ϕ are determined via least squares methods by fitting the data $u(x, z, t)$ to the model,

$$u(x,z,t) = u_0(x,z)\,\sin[\omega_{M_2} t + \phi_u(x,z)], \qquad (2)$$

where ω_{M_2} is the semidiurnal tidal frequency. Sensitivity studies were conducted by also fitting mean flow and a diurnal component to the flow. Neither significantly altered the M_2 solutions.

Example fits are shown in Figs. 3b,c for a region dominated by the semidiurnal internal tide (Fig. 3b) and one less so (Fig. 3c). Observations (x's and o's) and the resulting fit (black line) are plotted versus M_2 phase. Phase is relative to the beginning of the first cruise (29 June 2010) and does not correspond to high/low tide. Dashed lines in Fig. 3a and markers in Fig. 2 (top left) indicate their locations.

Our observations do not span the water column; thus, barotropic and baroclinic motions cannot be separated. Because the barotropic motions do not vary in depth and are laterally large scale, this choice does not affect the structure of the beams. Martin et al. (2006) found that the barotropic tides contributed <25% of the semidiurnal energy immediately above the ridge and <10% elsewhere.

The spatial structure of the M_2 beams is shown in Fig. 4 for observations (top panels) and the POM (bottom panels), for both amplitude (u_0; left panels) and a snapshot at time $t = t_o$ [$u_0 \sin(\omega t_0 + \phi_u)$; right panels]. Qualitative agreement is seen between the model and observations. Energy is seen extending downward from

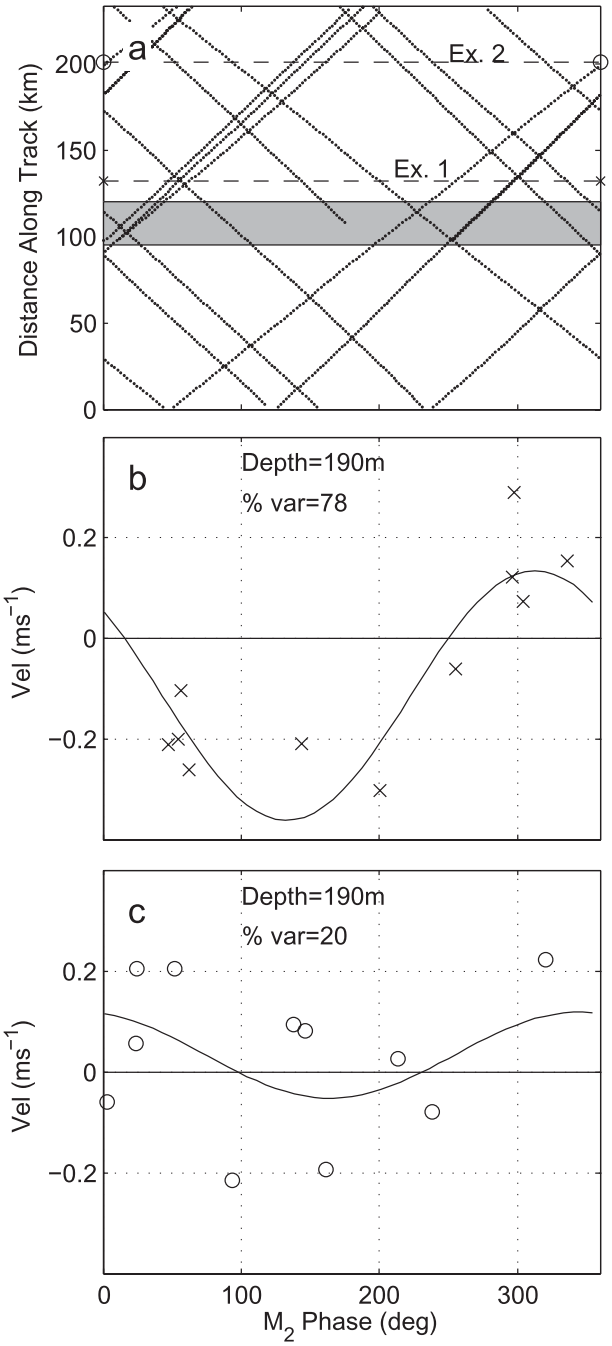

FIG. 3. The M_2 phase coverage and example time series. (a) The M_2 phase plotted vs distance along the transect. Gray shading indicates the location of Kaena Ridge along the ship track. Horizontal dashed lines in (a) indicate locations of (b),(c) example time series. Time series of measured along-track velocity and harmonic fit (line) for examples (b) 1 and (c) 2. The depth and percent of variance explained by the harmonic fit is also indicated.

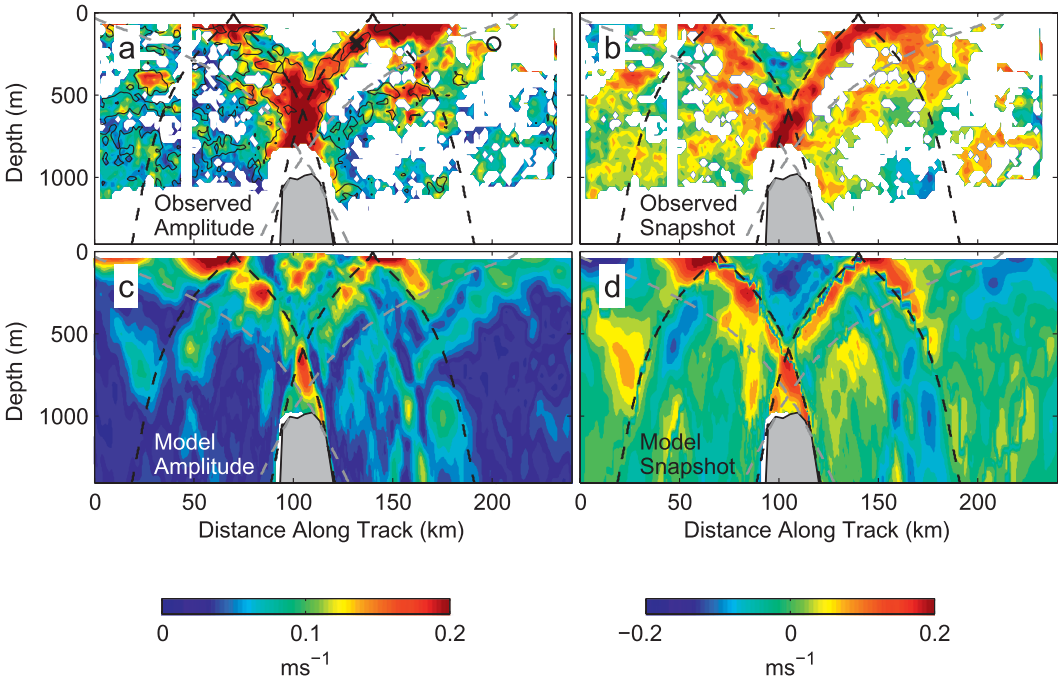

FIG. 4. Results of harmonic fit to velocity time series at each grid point: from observations, (a) M_2 amplitude (m s^{-1}) and (b) snapshot of M_2 velocity on yearday 179.4, constructed from harmonic fit. Data are contoured only where fit explained more than 20% of the variance. Black contours in (a) show regions where the fit explains greater than 60% of the variance. (c) Amplitude and (d) snapshot from POM along the ship track.

the northward surface bounce, as in the model. The observed amplitude is generally stronger than the model output, likely because the observations do not separate M_2 and S_2, whereas the model is M_2 only. The observations and the model both show elevated signals (i) at the intersection of the two beams above the ridge and (ii) near the first surface reflection.

4. Summary and discussion

Repeated opportunistic shipboard ADCP transects were conducted spanning Kaena Ridge, a major supercritical generator of internal tide beams. Harmonic fits were used to construct spatial maps of the structure of these beams and were then compared to theoretical characteristics and numerical model simulations. The depth range of the ADCP was 1000–1500 m compared to 600 m for previous studies by Martin et al. (2006) and Cole et al. (2009), revealing substantially more structure. The results from our harmonic fits generally agree with the model simulations and the previous observations.

The presence and location of the beams is relatively constant over time, as evidenced by the success of the harmonic fit to limited data spanning 10 months. However, individual sections do suggest some spatial variability between transects. Examination of spatial and temporal variations in stratification from both climatological data (Levitus and Boyer 1994) and Hawaii Ocean Time-Series data (http://hahana.soest.hawaii.edu/hot/hot-dogs/) indicate that they would shift the surface-reflection location by only 1–4 km. We hypothesize that spatial variations in the beams are due in large part to refraction by mesoscale currents, highlighting the need to better understand these effects on internal tides.

Additional interesting features were observed in the individual sections that were suggestive of near-diurnal internal tides, but our data were not sufficient to comment on them further. The database of *Kilo Moana* ADCP observations continues to grow with monthly trips to station Aloha. Future visitation of these additional data, when the time series is long enough to separate all the frequencies, may reveal more.

Acknowledgments. We are greatly thankful for the expertise, cheerful attitude, and hard work of the R/V *Kilo Moana* captain and crew. We also thank Jules Hummon and Eric Firing for their work maintaining the UHDAS ADCP acquisition and processing system. POM model results were kindly provided by Glenn Carter, Shaun Johnston, and Luc Rainville. We thank two anonymous reviewers for their helpful suggestions. This work was supported by NSF Grant OCE-0647971.

REFERENCES

Carter, G. S., and M. C. Gregg, 2006: Persistent near-diurnal internal waves observed above a site of M_2 barotropic-to-baroclinic conversion. *J. Phys. Oceanogr.,* **36,** 1136–1147.

Cole, S. T., D. L. Rudnick, B. A. Hodges, and J. P. Martin, 2009: Observations of tidal internal wave beams at Kauai Channel, Hawaii. *J. Phys. Oceanogr.,* **39,** 421–436.

Egbert, G., and S. Erofeeva, 2002: Efficient inverse modeling of barotropic ocean tides. *J. Atmos. Oceanic Technol.,* **19,** 183–204.

Lee, C. M., E. Kunze, T. B. Sanford, J. D. Nash, M. A. Merrifield, and P. E. Holloway, 2006: Internal tides and turbulence along the 3000-m isobath of the Hawaiian Ridge with model comparisons. *J. Phys. Oceanogr.,* **36,** 1165–1183.

Levitus, S., and T. Boyer, 1994: *Temperature*. Vol. 4, *World Ocean Atlas 1994,* NOAA Atlas NESDIS 4, 117 pp.

Martin, J. P., D. L. Rudnick, and R. Pinkel, 2006: Spatially broad observations of internal waves in the upper ocean at the Hawaiian Ridge. *J. Phys. Oceanogr.,* **36,** 1085–1103.

Merrifield, M., and P. Holloway, 2002: Model estimates of M_2 internal tide energetics at the Hawaiian Ridge. *J. Geophys. Res.,* **107,** 3179, doi:10.1029/2001JC000996.

Munk, W., and C. Wunsch, 1998: Abyssal recipes II: Energetics of tidal and wind mixing. *Deep-Sea Res. I,* **45,** 1977–2010.

New, A., and R. Pingree, 1992: Local generation of internal soliton packets in the central Bay of Biscay. *Deep-Sea Res.,* **39A,** 1521–1534, doi:10.1016/0198-0149(92)90045-U.

Rainville, L., and R. Pinkel, 2006: Propagation of low-mode internal waves through the ocean. *J. Phys. Oceanogr.,* **36,** 1220–1236.

——, T. M. S. Johnston, G. S. Carter, M. A. Merrifield, R. Pinkel, B. D. Dushaw, and P. Worcester, 2010: Interference pattern and propagation of the M_2 internal tide south of the Hawaiian Ridge. *J. Phys. Oceanogr.,* **40,** 311–325.

Rudnick, D., and Coauthors, 2003: From tides to mixing along the Hawaiian Ridge. *Science,* **301,** 355–357.

Wunsch, C., and R. Ferrari, 2004: Vertical mixing, energy and the general circulation of the oceans. *Annu. Rev. Fluid Mech.,* **36,** 281–314.